

Article

Blocking IbmiR319 impacts plant architecture and reduces drought tolerance in sweet potato

Lei Ren ^{1,2,#}, Tingting Zhang ^{1,2,#}, Haixia Wu ^{1,2}, Xinyu Ge ^{1,2}, Huihui Wan ^{1,2}, Shengyong Chen ⁴, Zongyun Li ^{1,2,*}, Daifu Ma ^{3,*}, Aimin Wang ^{1,2,*}

¹ Institute of Integrative Plant Biology, School of Life Science, Jiangsu Normal University, Xuzhou 221116, Jiangsu Province, People's Republic of China

² Jiangsu Key Laboratory of Phylogenomics & Comparative Genomics, School of Life Science, Jiangsu Normal University, Xuzhou 221116, Jiangsu Province, People's Republic of China

³ Xuzhou Institute of Agricultural Sciences in Jiangsu Xuhuai District, Key Laboratory for Biology and Genetic Breeding of Sweetpotato (Xuzhou), Ministry of Agriculture/Jiangsu Xuzhou Sweetpotato Research Center, 221131, People's Republic of China

⁴ Zhanjiang Academy of Agricultural Sciences, Zhanjiang Guangdong 524094, People's Republic of China

These authors contributed equally to this paper

* Correspondence: aiminwang@jsnu.edu.cn (A.W.), daifuma@163.com (D.M.), zongyunli@jsnu.edu.cn (Z.L.); Tel.: +86 516 83400033 (A.W.), +86 516 82189200 (D.M.), +86 516 83400033 (Z.L.)

Abstract: MicroRNA319 (miR319) plays a key role in plant growth, development, and multiple resistance by repressing the expression of targeted *TEOSINTE BRANCHED/CYCLOIDEA/PCF* (TCP) genes. Two members, *IbmiR319a* and *IbmiR319c*, were discovered in the miR319 gene family in sweet potato (*Ipomoea batatas* [L.] Lam). Here, we focused on the biological function and potential molecular mechanism of the response of *IbmiR319a* to drought stress in sweet potato. Blocking *IbmiR319a* in transgenic sweet potato (MIM319) resulted in a slim and tender phenotype and greater sensitivity to drought stress. Microscopic observations revealed that blocking *IbmiR319a* decreased the cell width and increased stomatal distribution in the adaxial leaf epidermis, and also increased the intercellular space in the leaf and petiole. We also found that the lignin content was reduced, which led to increased brittleness in MIM319. Quantitative real-time PCR showed that the expression levels of key genes in the lignin biosynthesis pathway were much lower in the MIM319 lines than in the wild type. Ectopic expression of *IbmiR319a*-targeted genes *IbTCP11* and *IbTCP17* in *Arabidopsis* resulted in similar phenotypes as MIM319. We also showed that the expression of *IbTCP11* and *IbTCP17* was largely induced by drought stress. Transcriptome analysis indicated that cell growth-related pathways, such as plant hormonal signaling, were significantly downregulated with the blocking of *IbmiR319a*. Taken together, our findings suggest that *IbmiR319a* affects plant architecture by targeting *IbTCP11/17* to control the response to drought stress in sweet potato.

Keywords: sweet potato; microRNA319; TCP transcription factor; drought stress.

Citation: Lastname, F.; Lastname, F29
Lastname, F. Title. *Genes* **2022**, *13*, x30
<https://doi.org/10.3390/xxxxx>

Academic Editor: Firstname Last-
name

Received: date
Accepted: date
Published: date

Publisher's Note: MDPI stays neu-
tral with regard to jurisdictional
claims in published maps and institu-
tional affiliations.



Copyright: © 2022 by the authors.
Submitted for possible open access
publication under the terms and
conditions of the Creative Commons
Attribution (CC BY) license
(<https://creativecommons.org/licenses/by/4.0/>).

1. Introduction

Drought is a major environmental factor causing abiotic stress (Pearce and RS 2001, Xie, Wang et al. 2017, Meng, Li et al. 2018). Severe drought restricts crop growth and significantly reduces yield worldwide (Burke, Lobell et al. 2009), (Hu and Xiong 2014). It is therefore essential that crops with drought tolerance traits are produced. Generally, the responses of plants to abiotic stress are similar, especially in the first phase—a rapid, osmotic phase that inhibits shoot growth (Zhou, Li et al. 2014). At the physiological level, the symptoms of drought damage include wilting, growth retardation through reduced photosynthetic capacity (especially the lost function of PSII) (Lin, Chiang et al. 2011), discoloration, abnormal ripening, and so on (Sato, Murakami et al. 2001).

Although sweet potato (*Ipomoea batatas* [L.] Lam) is a drought tolerant root crop, dry matter accumulation and root tuber enlargement are inhibited under drought stress, which seriously hampers production (Motsa, Modi et al. 2015). Genetic engineering methods can be used to improve drought tolerance. At the molecular level, the ectopic expression of enzyme genes, such as *XvSap1* (*Xerophyta viscosa* stress-associated proteins) (Mbinda, Dixelius et al. 2019), *SoBADH* (Spinach betaine aldehyde dehydrogenase) (Fan, Zhang et al. 2012), *AgcodA* (*Arthrobacter globiformis* choline oxidase), *AtHDG11* (*Arabidopsis* Homeodomain glabrous 11) (Long, Ruan et al. 2011), and *XvAld1* (*Xerophyta viscosa* Aldose reductase) (Mbinda, Ombori et al. 2018), improves drought tolerance in sweet potato. Overexpression of endogenous enzyme genes and structural genes, such as *IbC4H* (cinnamate 4-hydroxylase) (Wang, Zhu et al. 2017), *IbMIPS1* (myo-inositol-1-phosphate synthase) (Zhai, Wang et al. 2016), *IbCBF3* (dehydration-responsive element-binding/C-repeat-binding factor) (Jin, Kim et al. 2017), *IbNHX2* (Na^+/H^+ antiporters) (Wang, Zhai et al. 2016), *IbBT4* (BTB-TAZ-domain protein) (Zhou, Zhai et al. 2020), *IbARF5* (auxin response factor) (Kang, He et al. 2018), or transcription factors such as *IbZIP1* (basic region/leucine zipper motif transcription factor) (Kang, Zhai et al. 2019), *IbABF4* (abscisic acid (ABA)-responsive element binding factors) (Wang, Qiu et al. 2019), and *IbMYB116* (Zhou, Zhu et al. 2019), can also improve the drought tolerance of transgenic sweet potato plants.

The above studies mainly focused attention on maneuvering downstream gene functioning in the physiological responses of osmotic or ionic adjustment in sweet potato. The upstream regulatory networks of stress responses in sweet potato are still largely unknown. As we all know, microRNAs (miRNAs) involved in various plant stress responses through regulating their target genes, which are mainly transcription factors, forming a complex regulatory network and playing key roles in the gene regulation networks (Schommer, Palatnik et al. 2008). MiRNAs are small single-stranded, non-protein-coding RNAs of usually 20–24 nucleotides (nt) in length (Chen and Xuemei 2009, Taylor, Tarver et al. 2014) that regulate gene expression by mRNA cleavage at the post-transcriptional level or translational repression through base pairing with the complementary sequence within the target mRNAs involved in plant growth, development, and also various plant stress responses (Axtell, Snyder et al. 2007). MicroRNA319 (miR319) belongs to one of the most ancient and conserved miRNA families (Sunkar and R. 2004). More and more studies have shown that miR319 targets transcription factor *TCP* genes, playing vital roles in plant morphogenesis and reproduction (Palatnik, Allen et al. 2003, Jones-Rhoades, Bartel et al. 2006, Schommer, Debernardi et al. 2014), and also responding to multiple biotic and abiotic stresses (Yang, Dayong et al. 2013, Sun-ting, Xiao-li et al. 2014, Liu, Li et al. 2019, Fan, Ran et al. 2020). In leaf development, the overexpression of miR319 or suppression of its target *TCP* genes contributed to directly regulate the progression of the cell cycle genes *ICK1/KRP1* to control the G₂-M phase of the cell cycle (Schommer, Debernardi et al. 2014), causing an uneven leaf shape and curvature and resulting in serrated leaves in *Arabidopsis* (Palatnik, Allen et al. 2003). The miR319-TCP module also affects the balance between mitosis and endoreduplication (Wang, Tao et al. 2015). In the response to various stresses, overexpressing *shamiR319d* enhanced temperature tolerance by inhibiting the expression of *GAMYB-like1* and further altering temperature and reactive oxygen species (ROS) signal transduction in tomato (Shi, Jiang et al. 2019). The overexpression of both *OsaMIR319a* and *OsaMIR319b* led to enhanced cold tolerance by downregulating *OsPCF5* and *OsPCF8* in rice (Yang, Li et al. 2013). *PvmiR319*, targeting *PvPCF5*, promoted ethylene (ET) synthesis to improve salt tolerance in switchgrass (*Panicum virgatum* L.) (Liu, Li et al. 2019). The miR319a/TCP module participated in trichome initiation synergistically with gibberellic acid (GA) signaling and improved insect defenses in *Populus tomentosa* (Fan, Ran et al. 2020).

Although miR319-mediated changes in plant morphology and the response to biotic and abiotic stresses have been well studied in many plants, there is limited information available for sweet potato, which is a widely cultivated and important tuberous crop. In this study, we explored the function of the miR319-TCP module in plant architecture and

the tolerance to drought in sweet potato. We produced transgenic sweet potato plants with inhibited *IbmiR319a* by miRNA target MIMICS (MIM319) proven to be efficient in inhibiting miRNA function (Franco-Zorrilla, Valli et al. 2007). Blocking *IbmiR319a* not only affected plant architecture, but also reduced drought tolerance in sweet potato seedlings. Moreover, *IbTCP11/17*, two target genes of *IbmiR319a*, were participated in drought stress. Collectively, the results suggest that the miR319-IbTCP module modulates plant architecture, thereby influencing drought tolerance in sweet potato.

2. Materials and methods

Plant materials

The sweet potato cultivar ‘Xushu 22’ wild type (WT), developed by the Sweet Potato Research Institute of the China Agriculture Academy of Science (SPRI-CAAS), was used as a donor for genetic transformation. Untransformed and transgenic plants subcultured from *in vitro* plantlet cultures were transferred into plastic pots (18 cm in diameter) containing dark soil and vermiculite at a ratio of 2:1 (v/v) and grown in a growth chamber under a 16 h light/8 h dark photoperiod at $25 \pm 3^\circ\text{C}$. Shoots that were 3–4 cm in height were transplanted into the field in early May in 2020 for evaluation of the phenotype and agronomic traits at the Xuzhou experimental station (E $117^\circ 17.48'$, N $34^\circ 16.95'$) of the Sweet Potato Research Institute of the Chinese Academy of Agricultural Sciences (SPRI-CAAS).

The *A. thaliana* plants were grown in an artificial climate chamber at $22 \pm 3^\circ\text{C}$ and 16 h light/8 h dark photoperiod.

Plasmid and sweet potato genetic transformation

p35S-MIM319, the miR319 target mimicry vector, was constructed as previously described (Franco-Zorrilla, Valli et al. 2007). Genetic transformation of sweet potato was conducted according to the previously described method by Yang (Yang, Bi et al. 2011).

Vector construction and Arabidopsis transformation

The full-length CDSs of the *IbTCP11/17* sequences were amplified using gene-specific primers, and then cloned into the *SacI* and *KpnI* sites of the binary vector pCambia1300 containing the cauliflower mosaic virus 35S promoter to create the overexpression vectors IbTCP11OE and IbTCP17OE, respectively, and then transferred into *Agrobacterium tumefaciens* strain LBA4404. *Arabidopsis* transformation was performed using the floral-dip method to produce transgenic *Arabidopsis* plants (Clough and Bent 1998), which were subsequently grown in pots to produce T₃ seeds by screening with 50 mg/L hygromycin.

RNA isolation and qRT-PCR analysis

Total RNAs were extracted using TRIzol (Invitrogen) and then treated with RNase-free DNase I (Sigma) to remove contaminated genomic DNA. The RNA integrity was determined by 1% gel electrophoresis, and RNA concentration was measured using a NanoDrop spectrophotometer (ND1000, Technologies).

For quantitative real-time PCR (qRT-PCR) analyses of mRNA for the genes, 2 µg RNA per sample was reverse-transcribed to produce cDNA using the First Strand cDNA Synthesis Kit (Takara). The qRT-PCR was performed with the SYBR Green Real-time PCR Master Mix Kit (Takara), and the *IbActin* gene was used as an internal control. Data from three biological samples were collected, and the mean values were normalized to *IbActin*.

For miRNA quantitative analysis, the stem-loop RT-PCR method was used. One microgram of DNase-treated RNA was converted into cDNA using the First Strand cDNA Synthesis Kit (Takara). The miR319-specific primer and miRNA universal primer (URP) were used for qRT-PCR. *IbActin* RNA was used as an endogenous control. The abundance of *miR319* was normalized to *IbActin* RNA as a reference.

The relative abundance of gene expression was determined using the $2^{-\Delta\Delta C_t}$ method (Livak and Schmittgen 2001). All gene expression data are from three biological replicates with three technical replicates for each biological sample. The sequences for the primers are listed in Supplementary Table S1.

Microscopic observations

For paraffin sectioning, the first fully expanded fresh leaves or stems were fixed in 0.1 M sodium phosphate buffer containing 2.5% (v/v) glutaraldehyde for 24 h. Samples were dehydrated through an alcohol series, followed by resin-alcohol grading and embedding in acrylic resin. Semi-thin sections of 1 mm thickness were obtained using standard rotary microtomy technique and stained with Safranin O-Fast Green. Photomicrographs were taken under 10× and 20× objectives of the fluorescence microscope (Axiolab, Zeiss, MC80 Dx Camera).

For epidermis cell observation, the first fully expanded fresh leaves were folded and torn gently from the fold, and a small piece of torn white film was made into a temporary slide and observed with a light microscope. The length and width of the epidermis cells were measured, and the stoma were counted.

Lignin deposition experiment and lignin content measurement

Analysis of the Klason lignin content was performed with the sulfuric acid digestion method (Hatfield, Jung et al. 1994). For lignin deposition staining with toluidine blue, hand-cut sections of the third internode were cut from two-month-old plants in the greenhouse. Free-hand slices were made and stained with toluidine blue (toluidine blue staining solution, Servicebio) for about 2 min, rinsed with water, and then observed under an optical microscope.

Measurement of breaking force

The third internodes from the top of two-month-old MIM319 and WT seedlings were used for measurements. The force required to break the stems was recorded with a texture analyzer (Shimadzu, EZ Test, Japan) with the detector TA52. Ten plants of each of MIM319 and WT were measured, and all measurements were taken under the same conditions.

Analysis of drought tolerance

The cuttings of MIM319 and WT were used for drought stress experiments. The cuttings transplanted for 2 weeks were watered sufficiently for one week, following water was withheld for 4 weeks to simulate drought stress. The physiological indexes, including malondialdehyde (MDA) and proline contents, and antioxidant enzyme system activity, were measured with assay kits (Nanjing Jiancheng Bioengineering Institute, Nanjing, China) as described before (Wang, Zhu et al. 2017). Each data point was the average of three replicates. Approximately 20 cuttings of each line were used for each experiment, and at least three replicates of each experiment were performed, and the results were consistent. The result from one set of experiments is presented herein.

Gene expression analysis

The first fully expanded leaves of MIM319 and WT plants subjected to drought stress for one week were used to analyze relative expression level of the genes related to stress responses, including proline biosynthesis and the ROS-scavenging system, using qRT-PCR. The sequences of the specific primers are listed in Supplementary Table S1.

Transcriptome analysis

Total RNA was extracted from the shoots of MIM319 and WT grown in a transplanting box for 4 weeks using the TRIzol method (Invitrogen, Carlsbad, CA), and 1 g RNA was

used for Illumina RNA-Seq. Transcriptome sequencing and *de novo* transcriptome assembly and evaluation were performed by Huada (Beijing, China). After filtering with SOAP-nuke (v1.5.2) (<https://github.com/BGI-flexlab/SOAPnuke>), clean reads were obtained and stored in FASTQ format. The clean reads were mapped to the reference genome using HISAT2 (v2.0.4) (<http://www.ccb.jhu.edu/software/hisat/index.shtml>). Bowtie2 (v2.2.5) (<http://bowtiebio.sourceforge.net/20Bowtie220/index.shtml>) was used to align the clean reads to the reference coding gene set, and then the expression level of the genes was calculated by RSEM (v1.2.12) (<https://github.com/deweylab/RSEM>). A heatmap was produced using pheatmap (v1.0.8) (<https://cran.r-project.org/web/packages/pheatmap/index.html>) according to the gene expression in different samples. The differential expression analysis was performed using DESeq2 (v1.4.5) (<http://www.bioconductor.org/packages/release/bioc/html/DESeq2.html>) with Q-values ≤ 0.05 . Gene Ontology (GO; <http://www.geneontology.org/>) and Kyoto Encyclopedia of Genes and Genomes (KEGG; <https://www.kegg.jp/>) enrichment analyses of differentially expressed genes (DEGs) were performed by Phyper (https://en.wikipedia.org/wiki/Hypergeometric_distribution) based on the hypergeometric test. The significance levels of the terms and pathways were corrected by the Q-value with a rigorous threshold (Q value ≤ 0.05) by Bonferroni (Abdi 2007).

Statistical analysis

Student's *t*-test was used to analyze all the data presented as the mean \pm SE. *P*-values of < 0.01 , or < 0.05 were considered to be statistically significant.

Results

Identification and characterization of *IbmiR319* in sweet potato

MiR319 was the first miRNA identified through positive genetic screening (Palatnik, Allen et al. 2003). In previous studies, we constructed a miRNA library of sweet potato based on high-throughput sequencing (Xie, Wang et al. 2017), and two members of the miR319 family (*IbmiR319a* and *IbmiR319c*) with different matured miRNA sequences were found (Fig. 1A, B). Both *IbmiR319* precursors were supported by cDNAs in the public database (<http://public-genomes-ngs.molgen.mpg.de/SweetPotato/>). The gene encoding *IbmiR319a* was located in chromosome (chr) 15 from 18892867 to 18893043 (Supplement Fig. 1A), while that of *IbmiR319c* was located in chr 2 from 47619325 to 47619514 (Supplement Fig. 1B).

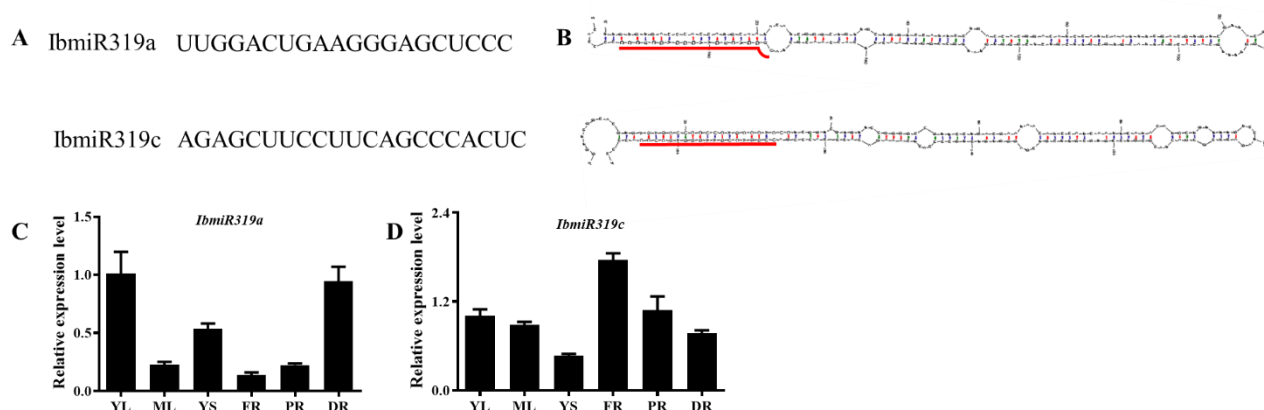


Figure 1. The microRNA319 family contains two members in sweet potato. **A:** Sequence of mature *IbmiR319a* and *IbmiR319c*. **B:** The secondary structure of the precursor sequence of *IbmiR319a* and *IbmiR319c*. **C, D:** The expression patterns of *IbmiR319a* and *IbmiR319c*. YL: young leaf; ML: mature leaf; YS: young stem; FR: fibrous root; PR: pencil root; DR: developing root.

To determine the expression patterns of *IbmiR319*, we conducted stem-loop qRT-PCR of *IbmiR319* mature transcripts in the leaves, stems, fibrous roots, pencil roots, and storage roots (Fig. 1C, D). *IbmiR319a* showed a higher expression level in the young organs or vigorously growing organs, especially the young leaf and developing root, while *IbmiR319c* showed a higher expression level in the fibrous roots, indicating that *IbmiR319a* may play an important role in development. We therefore focused our attention on the functional analysis of *IbmiR319a*.

Generation of transgenic sweet potato plants with *miR319a* blocked

To investigate the function of *IbmiR319a* in sweet potato, we constructed a plasmid overexpressing *IbmiR319a* target mimicry (MIM319), intending to sequester the normal expression of native *IbmiR319a*, and transformed it into the sweet potato variety 'Xu22', which was used as WT. We obtained seven independent transgenic MIM319 plants, among which five positive plants named m3-2, m3-3, m3-8, m3-9, and m3-10 were verified (Supplement Fig. S2A–D). To determine the expression level of *IbmiR319a*, these five positive transgenic lines were analyzed using stem-loop qRT-PCR, with WT as the control. The abundance of *IbmiR319a* mature transcripts in transgenic plants was lower than that in WT (Fig. 2A), suggesting that the MIM319 fusion plasmids were successfully expressed in sweet potato, and normal *IbmiR319a* was successfully blocked. Two independent transgenic lines m3-8 and m3-9, with relatively lower *IbmiR319a* expression levels, were chosen for further analysis.

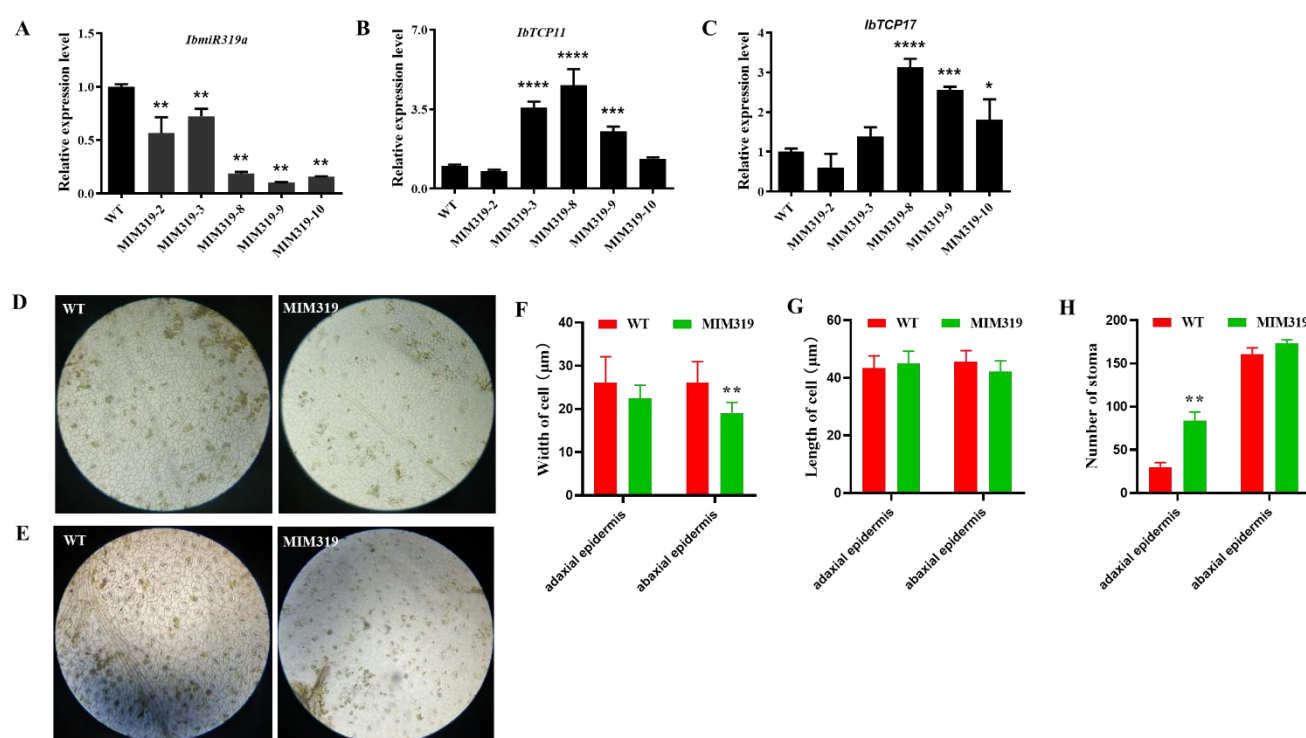


Figure 2. Light microscopic observation of MIM319 transgenic sweet potato plants. **A:** Expression level of mature *IbmiR319a* in MIM319 transgenic sweet potato lines and WT. **B, C:** Expression level of the target genes *IbTCP11/17* in MIM319 transgenic sweet potato lines and WT. **D:** Images of leaf adaxial epidermal cells of the WT and MIM319 plants under the light microscope. **E:** Images of leaf abaxial epidermal cells of the WT and MIM319 plants under the light microscope. **F:** Quantitative measurement of the maximum leaf epidermis cell width of WT and MIM319 transgenic plants (n=100). **G:** Quantitative measurement of the maximum leaf epidermis cell length of WT and MIM319 lines (n=100). **H:** Statistical analysis of total stomata number in WT and MIM319 transgenic plants (n = 30). Data are presented as means ± SE, and error bars represent SE. Asterisks indicate significant differences between transgenic and control plants at $P < 0.01$ by Student's *t*-test.

Expression level of the putative *IbmiR319a* target genes was upregulated in MIM319 transgenic sweet potato

In general, miRNAs play important roles by post-transcriptionally regulating their target genes. In sweet potato, *IbmiR319a* was predicted to target Transcript comp94376_c4 and comp87184_c3 according to our degradation and transcriptome sequencing results (Xie, Wang et al. 2017). Using these sequences as a reference in the BLAST search in the genomics database for its two wild ancestors (*Ipomoea trifida* and *Ipomoea triloba*) (<http://sweetpotato.uga.edu/>), we found that they were 98% identical to sequence ID CP025644.1 on chr 1 and CP025653.1 on chr 10 of *I. trifida* (Supplement Fig. S3A, B). We named them *IbTCP11* and *IbTCP17* according to their chromosome location (Ren, Wu et al. 2021). The complementary area between the targets and *IbmiR319a* was shown in our previous study through the psRNA Target tool (Ren, Wu et al. 2021). We further checked the predicted *IbTCP11* and *IbTCP17* transcript levels in MIM319 plants by qRT-PCR. The result showed that *IbTCP11/17* increased the mRNA levels in the leaves of transgenic MIM319 plants compared to the WT (Fig. 2B, C). Considering that MIM319 plants showed a relatively low level of mature *IbmiR319a* expression in the leaves where the miR319-targeted *IbTCP11/17* had a high level of expression, we assumed that blocking *IbmiR319a* could promote the high mRNA levels of the targeted genes.

Blocking *IbmiR319a* in sweet potato caused pleiotropic phenotype changes

As previously reported, the highly conserved ancient miR319 plays an important role in plant development (Yang, Dayong et al. 2013). Moreover, overexpressing or blocking *miR319* resulted in pleiotropic phenotype changes. All positive MIM319 transgenic sweet potatoes blocking *IbmiR319a* showed similar phenotypes. Despite the narrow and small leaves previously reported (Ren, Wu et al. 2021), a more thorough investigation was conducted. Microscopic analysis of the leaf samples showed that the epidermal cells of MIM319 were shaped like irregular squares, while the WT cells were irregular rectangles (Fig. 2D, E). The average length of the adaxial and abaxial leaf epidermis cells was 45 μm and 42.22 μm in MIM319, respectively, which was not obviously different from that of the WT (43.33 μm and 45.56 μm , respectively). However, the average width of the abaxial and adaxial leaf epidermis cells was 19.11 μm and 22.56 μm in MIM319, which was dramatically different from that of WT at 26.11 μm (Fig. 2F, G). Meanwhile, the number of stoma was increased, especially that of the adaxial leaf epidermis, which was 84 per microscopic view in MIM319, indicating a significant increase compared with the WT (30 per microscopic view) (Fig. 2H). A looser arrangement of mesophyll cells (including spongy tissue and palisade tissue) in the leaf transverse section (Fig. S4A) and larger intercellular spaces in the petiole transverse section was found compared to that of the WT (Fig. S4B).

From the whole plant level, the height of MIM319 was dramatically higher than that of WT in the greenhouse (Fig. 3A). After transplanting into an incubator for one month, the transgenic plants MIM319 were 14.48 cm tall, whereas the WT was only 9.07 cm (Fig. 3B). Blocking *IbmiR319a* also led to a decreased stem diameter in the transgenic plant MIM319. The diameter of the basal stem of the transgenic plant MIM319 was 1.987 mm, which was much slenderer than that of WT at 3.62 mm (Fig. 3C).

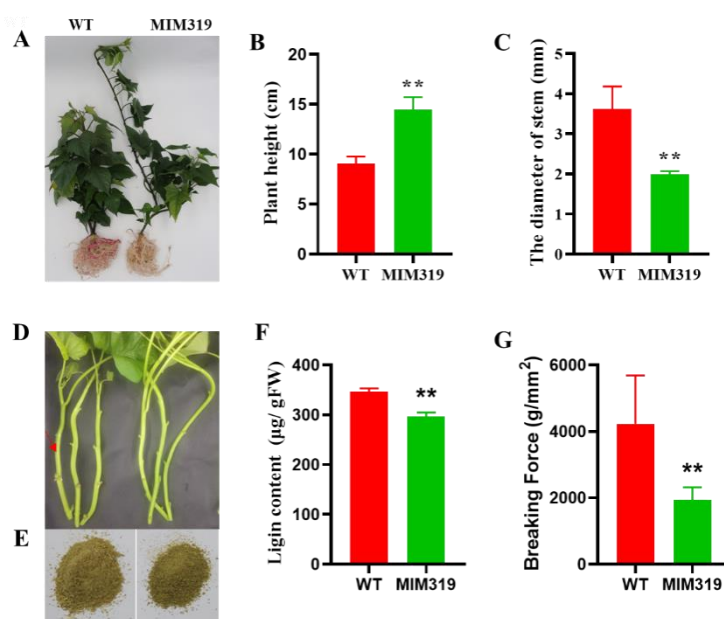


Figure 3. Phenotypes of MIM319 transgenic sweet potato plants. **A:** The transgenic plants (MIM319) exhibited increased plant height and decreased stem diameter compared to the WT controls. **B:** Statistical analysis of plant height in MIM319 transgenic plants and WT ($n = 20$). **C:** Statistical analysis of stem diameter in MIM319 transgenic plants and WT ($n = 20$). **D:** A closer look at the MIM319 transgenic plants and WT. The representative transgenic plant stem is slender. The red arrow indicates the sample location. **E:** Powdered stems of MIM319 (left) and WT (right). **F:** Statistical analysis of lignin content in WT and MIM319 transgenic plants ($n = 10$). **G:** The breaking force of the stems in the WT and MIM319 transgenic plants ($n = 20$). Data are presented as means \pm SE, and error bars represent SE. Asterisks indicate significant differences between transgenic and control plants at $P < 0.01$ by Student's t -test.

During planting, we found that the stems of MIM319 were more brittle and broke easily. We further determined the lignin content, deposition, and the load capacity of the stems. Under the same grinding conditions, the stem powder of MIM319 was finer than that of WT (Fig. 3D, E). Furthermore, the total Klason lignin content of MIM319 was 296.10 $\mu\text{g/gFW}$, which was ~~dramatically~~ decreased compared to the 346.45 $\mu\text{g/gFW}$ in WT (Fig. 3F). Toluidine blue staining for lignin in the third internodes also revealed a lower number of lignified cells around the xylem, as indicated by the decreased coloration in comparison with the WT (Fig. S5A). Less purplish-red staining by saffron was observed in the vertical section of MIM319 stems than that in WT (Fig. S5B). The breaking force of MIM319 was 1938 g/mm^2 , which was also significantly less than 4226.67 g/mm^2 in WT (Fig. 3G).

All these findings suggest that blocking *IbmiR319a*, with the resulting upregulation of *IbTCP11/17*, caused alterations in growth and development and lignin content in sweet potato.

RNA-Seq analysis of transgenic sweet potato plants with blocked *IbmiR319a*

To explore the potential molecular mechanisms affecting growth and development in MIM319 plants, RNA-Seq analysis was performed using the shoots of the MIM319 lines (m3-8 and m3-9) and WT. The DEGs were identified based on adjusted P -values < 0.05 . To validate the RNA-Seq data, the expression of 10 randomly selected DEGs was examined by qRT-PCR and was found to be consistent with that determined by RNA-Seq (Fig. S6). The RNA-Seq results identified 5587 DEGs between MIM319 and WT plants, including 3119 upregulated and 2468 downregulated genes (Fig. 4A, Supplementary Table S2). The GO functional annotation of the DEGs revealed that blocking *IbmiR319a* affected multiple biological processes, including developmental process, growth, metabolic process, and signal transduction (Fig. 4B, Supplementary Table S3). The KEGG pathway analysis showed that 116 DEGs were enriched in MAPK signaling transduction, and 80 DEGs were

enriched in phenylpropanoid biosynthesis (Fig. 4C, Supplementary Table S4). For example, the transcript CL5843.Contig1_Ib, which is homologous to longifolia1-like, functions in regulating leaf morphology by promoting cell expansion in the leaf-length direction (Lee, Kim et al. 2006, Lee and Kim 2018). The mutant of transcript CL431.Contig8_Ib, which is homologous to E3 ubiquitin-protein ligase DIS1, was defective in trichome cell expansion and actin organization, resulting in a distorted trichome phenotype (Zou, Zheng et al. 2016) in *Arabidopsis*. Transcript CL11749.Contig1_Ib, defined as a SAUR family protein, plays a central role in auxin-induced acid growth (Stortenbeker and Bemer 2019, Wang, Sun et al. 2020).

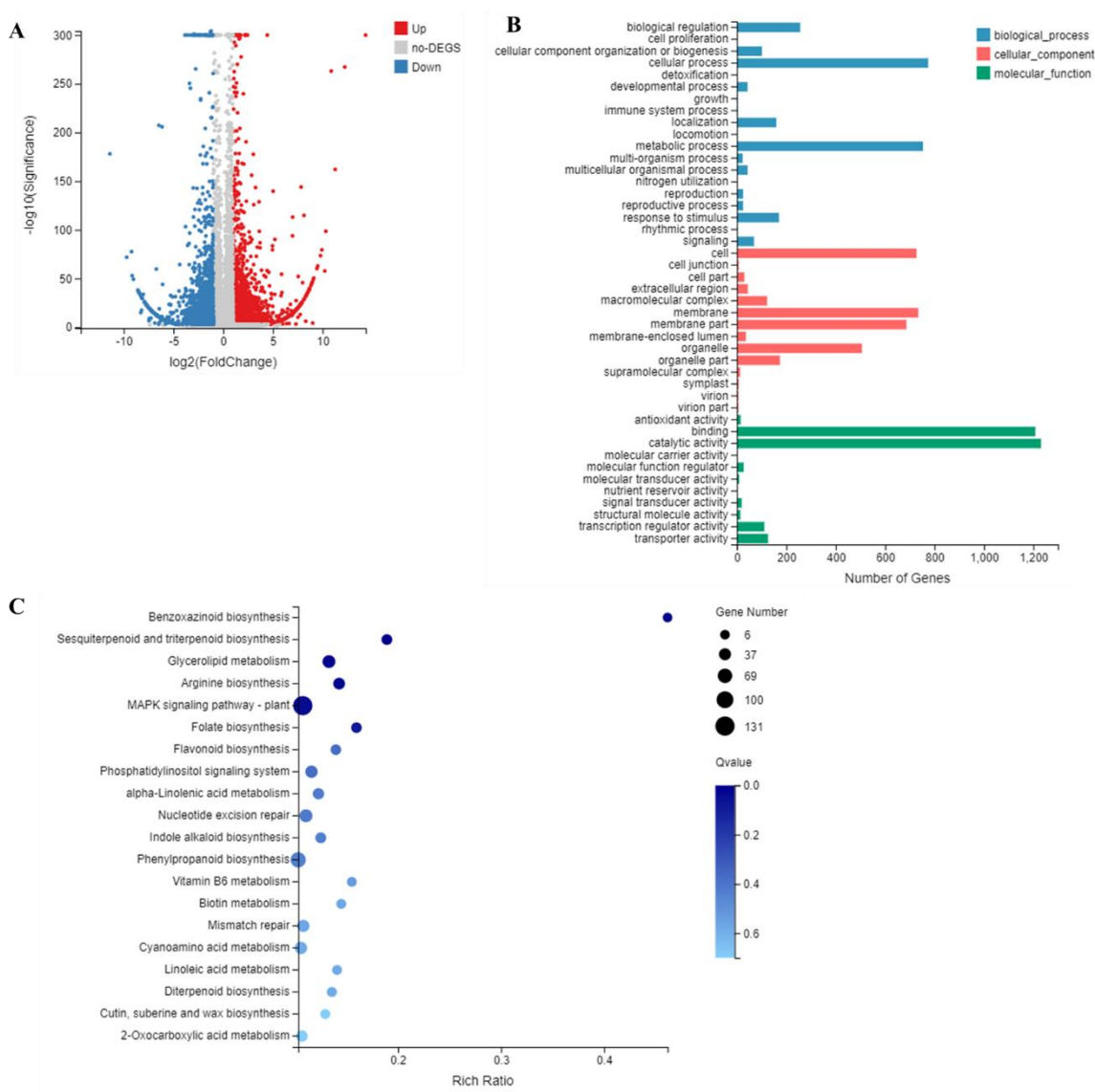


Figure 4. RNA-Seq analysis of MIM319 transgenic sweet potato and WT. **A:** Volcano plot shows the differentially expressed genes (DEGs) between MIM319 transgenic sweet potato and WT. Blue circles represent downregulated DEGs; red circles represent upregulated DEGs; and grey circles represent non-DEGs. **B:** GO analysis of the DEGs between MIM319 transgenic sweet potato and WT. **C:** KEGG pathway analysis of the DEGs between MIM319 transgenic sweet potato and WT.

Transgenic plants overexpressing IbTCP11 and IbTCP17 also had a narrow and small leaf phenotype and decreased lignin content

To further examine the function of *IbmiR319a*, a biological function analysis of *IbTCP11* and *IbTCP17* was conducted. We individually overexpressed each of these two

genes in *Arabidopsis*. Transgenic plants overexpressing *IbTCP11* (IbTCP11OE) and *IbTCP17* (IbTCP17OE) had narrow and small leaves, a decreased number of rosette leaves (Fig. 5A, B), and a decreased lignin content (Fig. 5C), and also resembled the MIM319 phenotype in sweet potato, in which *IbTCP11/17* were upregulated because of native *IbmiR319a* being blocked. The expression profile of these two target genes in various tissues was examined by qRT-PCR in our previous study (Ren, Wu et al. 2021). *IbTCP11/17* were highly expressed in the aboveground tissues, including the shoot bud, leaf, and stem, but they were weakly expressed in the belowground organs. The expression level of *IbTCP11/17* was relatively negatively correlated with the expression of *IbmiR319a*, at least in the shoot buds and leaves. These results suggest that these two target genes *IbTCP11/17* might be involved in the regulation of plant architecture and lignin content.

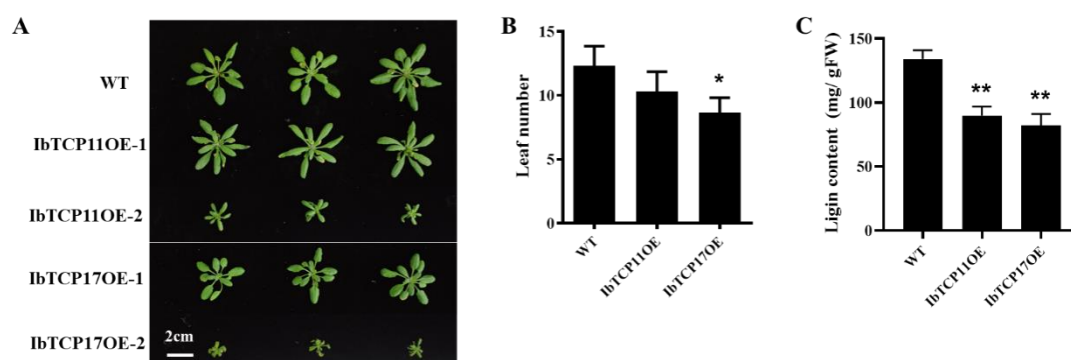


Figure 5. Phenotypes of transgenic *Arabidopsis* plants. **A:** The transgenic plants (IbTCP11-OE and IbTCP17-OE) exhibited a smaller plant structure and leaf than the WT controls. Photographs of representative seedlings of WT and two transgenic lines were taken. **B:** Statistical analysis of leaf number in IbTCP11OE and IbTCP17OE transgenic plants and WT (n = 20). **C:** Statistical analysis of lignin content in IbTCP11-OE and IbTCP17-OE transgenic plants and WT (n = 10).

Blocking *IbmiR319a* in sweet potato resulted in decreased drought tolerance

We wanted to assess whether blocking *IbmiR319a* would affect the performance of sweet potato under drought conditions due to morphological changes in the stems and leaves. MIM319 and WT plants with 3–4 mature leaves were subjected to drought for 4 weeks. All plants showed wilting, yellowing, and necrosis, although the leaves of MIM319 showed more severe withering than those of WT. After re-watering for two weeks, most WT plants survived, while the MIM319 transgenic plants perished (Fig. 6A).

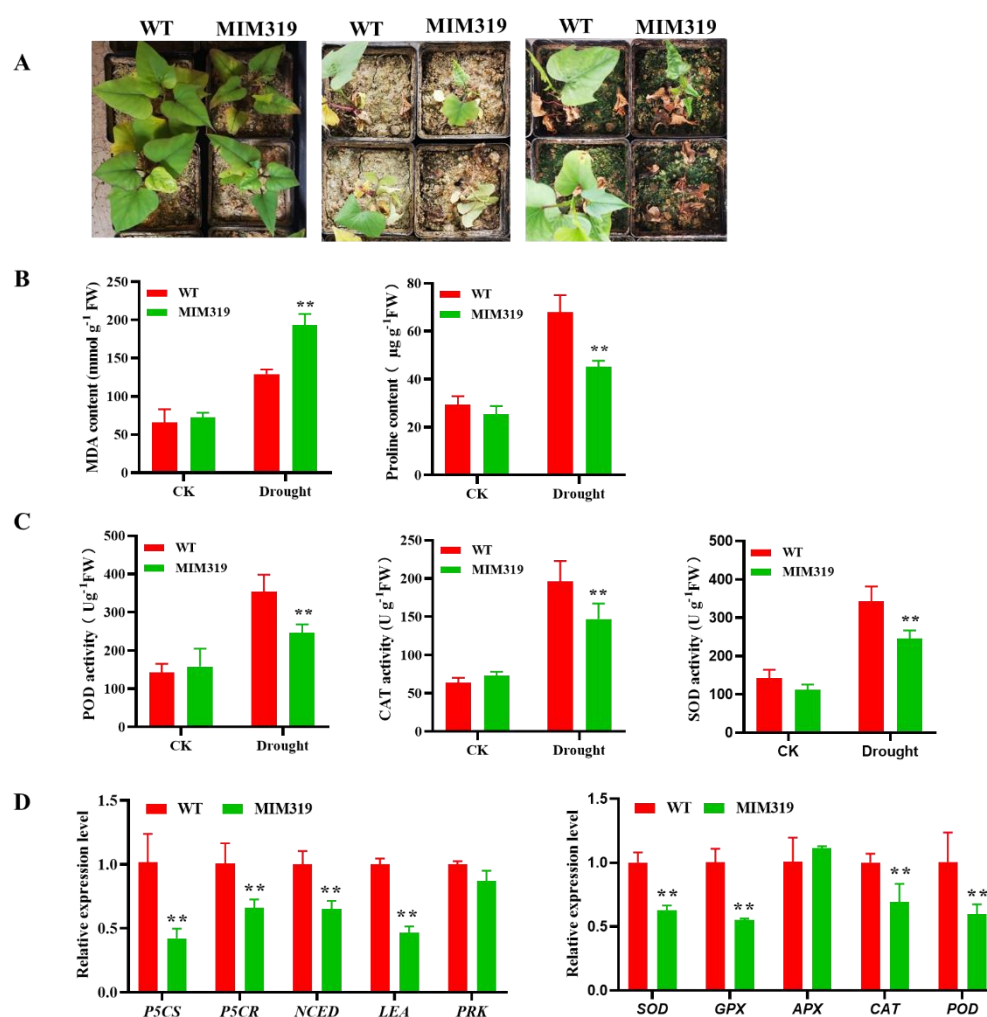


Figure 6. Drought tolerance analysis of MIM319 transgenic sweet potato plants. **A:** Phenotypes of MIM319 transgenic plants vs. WT grown for 6 weeks under normal conditions and 4 weeks under drought stress followed by 2 days re-watering after 2 weeks of normal treatment. **B:** MDA and proline contents in the MIM319 transgenic plants and WT grown for 2 weeks under drought stress after 2 weeks of normal treatment. **C:** Peroxidase (POD), catalase (CAT), and superoxide dismutase (SOD) activity in the MIM319 transgenic plants and WT grown for 2 weeks under drought stress after 2 weeks of normal treatment. **D:** Transcript levels of salt and drought responsive genes in leaves of MIM319 transgenic plants and WT plants that had been pot-grown for 4 weeks under normal conditions and 2 weeks under drought stress after 2 weeks of normal treatment. Each value is the mean of three biological repeats \pm the standard deviation (SD). Asterisks indicate significant differences between transgenic lines and WT. * $P < 0.05$; ** $P < 0.01$, Student's *t*-test.

The drought tolerance of the plants was further evaluated. No differences in the MDA contents between the MIM319 transgenic plants and WT were observed under control conditions (room temperature or normal watering). However, the MDA content of MIM319 increased by 2.65 and 2.9 times, respectively, under drought stress compared to normal conditions, whereas an increase of only 1.97 times was detected in WT (Fig. 6B).

An opposite pattern was observed for proline content. There was no difference in the proline contents between the MIM319 transgenic plants and WT under control conditions. By contrast, under drought treatment, the proline content of MIM319 was significantly increased by 1.77 and 1.94 times, respectively, which were all lower than the 2.3 times increase detected in WT (Fig. 6B).

Quantitative RT-PCR analysis was also used to detect the expression level of the drought stress-responsive genes. Well-known stress-responsive genes, including a proline biosynthesis-related gene encoding a pyrroline-5-carboxylatesynthase (*lbp5CS*) and pyr-

roline-5-carboxylate reductase (*IbP5CR*); an abscisic acid (Hirakawa, Okada et al.) biosynthesis-related gene encoding a zeaxanthin epoxidase (*IbZEP*); 9-*cis*-epoxycarotenoid dioxygenase (*IbNCED*); a late embryogenesis abundant protein (*IbLEA*); a photosynthesis-related gene encoding a phosphoribulokinase (*IbPRK*); and ROS scavenging-related genes encoding superoxide dismutase (*IbSOD*), peroxidase (*IbPOD*), catalase (*IbCAT*), ascorbate peroxidase (*IbAPX*), glutathione peroxidase (*IbGPX*), were significantly downregulated in the MIM319 transgenic plants compared to WT after two weeks of drought stress (Fig. 6C, D).

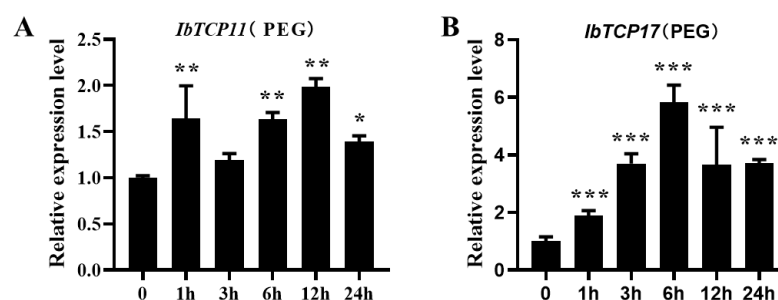


Figure 7. Expression analysis of the target genes *IbTCP11* (A) and *IbTCP17* (B) in the WT at different times (h) in response to 20% PEG. Data are presented as mean values \pm SE (n=3). * and **, *** indicate a significant difference compared to the WT at $P < 0.05$ and < 0.01 , < 0.0001 , respectively, based on Student's *t*-test.

These results implied that blocking *IbmiR319a* inhibited the antioxidant system, which includes the inhibited transcriptional expression and activity of the ROS-scavenging enzymes under drought stress.

IbmiR319a functions in plant tolerance to drought stress possibly by inhibiting *IbTCP11/17* expression in sweet potato

The expression level of *IbTCP11/17* in the WT sweet potato was more strongly induced by polyethylene glycol (PEG) 6000, which was used to simulate drought stress. The expression of *IbTCP11* peaked (2 times) at 12 h, while that of *IbTCP17* peaked (6 times) at 6 h. These results implied that *IbTCP11/17* might be involved in drought tolerance in sweet potato.

DISCUSSION

Although sweet potato is a root crop that is highly important for food security (Liu, Liu et al. 2014), research on sweet potato has lagged behind other crops, such as rice, wheat, and maize, because of the complexity of the genome and the inefficiency of genetic transformation. So far, the only functionally characterized miRNAs in sweet potato are *IbmiR2111* (Weng, Kuo et al. 2020), *IbmiR828* (Lin, Lin et al. 2012), and *IbmiR408* (Kuo, Lin et al. 2019). In the present study, we found that *IbmiR319a* negatively regulated the abundance of *IbTCP11/17* mRNA, which affected plant architecture and drought tolerance in sweet potato.

In sweet potato, the miR319 family has two members that are each encoded by *IbMIR319a* and *IbMIR319c*. A growing number of studies have reported that the function of miR319 is far ranging and conserved among different species (Zhou, Li et al. 2014, Liu, Li et al. 2019, Shi, Jiang et al. 2019, Cao, Zhao et al. 2020, Fan, Ran et al. 2020). The overexpression of *miR319* or downregulation of its target genes leads to a broader and crinkled leaf phenotype in transgenic dicotyledonous plants such as *Arabidopsis* (Palatnik, Allen et al. 2003) and tomato (Shi, Jiang et al. 2019), but only a broader leaf phenotype in transgenic monocotyledonous plants, such as rice (Yang, Dayong et al. 2013) and switchgrass (Xie, Liu et al. 2017). In our study, blocking *IbmiR319a* led to a narrow and small leaf phenotype

in transgenic sweet potato, which was the opposite phenotype to the overexpression transgenic plant. Blocking *IbmiR319a* also led to a decreased stem diameter in transgenic plants. These results suggest that the function of miR319 in leaf morphogenesis and plant growth is highly conserved in sweet potato.

AtTCP2, an orthologous gene of *IbTCP11*, interacts with *AtCRY1* to inhibit hypocotyl elongation under blue light (He, Zhao et al. 2016). The function of *CsnTCP2* was shown to be suppressed by *CsnmiR319c* in the bud dormancy-activity cycle in tea plant (Liu, Mi et al. 2019). *AtTCP2* also positively regulated the expression of *Circadian clock associated 1* (*CCA1*) and *EARLY FLOWERING 3* (*ELF3*) to affect leaf morphogenesis and flowering time and mediate the jasmonic acid (JA) signaling pathway to inhibit hypocotyl elongation (He, Zhou et al. 2021). *AtTCP4*, an orthologous gene of *IbTCP17*, directly activates *VND7* to participate in secondary cell wall biosynthesis and programmed cell death (Sun, Wang et al. 2017), and also directly activates *TRICHOMELESS1* (*TCL1*) and *TCL2* to suppress trichome initiation (Vadde, Challa et al. 2019). *AtTCP4* and *PIF3* antagonistically participate in photomorphogenesis and facilitate light-induced cotyledon opening in *Arabidopsis* (Dong, Sun et al. 2019). Among the 18 *IbTCP* genes in sweet potato, there are only four complementarily targeted by *IbmiR319* (Ren, Wu et al. 2021). Overexpression of the target genes *IbTCP11/17* in *Arabidopsis* (*IbTCP11OE*, *IbTCP17OE*) led to a narrow and small leaf phenotype and a decreased lignin content, which was consistent with that of *MIM319* in sweet potato.

Leaves are not only important photosynthetic plant organs but are also the interface for plant water metabolism (Tsukaya 2005). Water loss through stomatal transpiration is one of the key determinants of drought tolerance (Matsuda, Takano et al. 2016). The density and distribution of stomata directly affect plant water metabolism and drought tolerance. In our study, the leaf epidermal cells were slenderer and had more stomata in *MIM319* than in WT, and the mesophyll cells were more loosely arranged and the intercellular space was larger in *MIM319* than in WT; all of which may result in increased water loss and decreased drought tolerance.

Lignin is an important polymer of phenylpropanoid compounds and plays a vital role in biotic and abiotic stress tolerance in plants. Greater lignification improves drought resistance by increasing water retention capacity (Moura, Bonine et al. 2010, Pereira, Domingues et al. 2018). The overexpression of a rice HD-Zip transcription factor *OsTF1L* (Bang, Lee et al. 2019), foxtail millet (*Setaria italica*) R2R3-MYB transcription factor *SiMYB56* (Xu, Tang et al. 2020), or key genes in the lignin biosynthesis pathway, such as 4-coumarate-CoA ligases gene in *Gossypium hirsutum* (*Gh4CL7*) (Sun, Xiong et al. 2020), cinnamyl alcohol dehydrogenase gene in *Cucumis melo* L. (*CmCAD*) (Liu, Jiang et al. 2020), and caffeoyl-CoA O-methyltransferase gene in *Paeonia ostii* (*PoCCoAOMT*) (Zhao, Luan et al. 2021), can all significantly enhance tolerance to drought stress in transgenic plants by regulating lignin biosynthesis. In *Arabidopsis*, miR319-targeted *AtTCP4* activated *VND7* expression to increase lignin content in the secondary cell wall (Sun, Wang et al. 2017). In our study, blocking *IbmiR319a* led to increased brittleness and decreased lignin content, and as a result, reduced the drought tolerance in sweet potato.

Author Contributions: L.Ren, Z.Li, D.Ma, and A.Wang designed the research. L.Ren, T.Zhang, H.Wu, X.Ge, and H.Wan performed the experiments. Z.Li contributed to reagents, materials, and analysis tools. L.Ren, and A.Wang wrote the manuscript. Z.Li and D.Ma modified the manuscript. All authors contributed to the article and approved the submitted version.

Funding: This work was supported by the China Agriculture Research System of MOF and MARA (Grant No. CARS-10-B02), the National Key R&D Program of China (2018YFD1000705 and 2018YFD1000700), the Project of Xuzhou Science and Technology Key R&D Program (Grant No. KC21142), Postgraduate Research & Practice Innovation Program of Jiangsu Province (Grant No. KYCX21_2605), and the Research Innovation Program for College Graduates of Jiangsu Normal University (Grant No. 2020XKT497; 2021XKT0785), the Priority Academic Program Development of Jiangsu Higher Education Institutions (PAPD).

Acknowledgments: We thank LetPub (www.letpub.com) for its linguistic assistance during the preparation of this manuscript.

References

- Abdi, H. (2007). "The Bonferroni and Šidák Corrections for Multiple Comparisons." *encyclopedia of measurement & statistics* **1**: 1-9.
- Axtell, M. J., J. A. Snyder and D. P. Bartel (2007). "Common Functions for Diverse Small RNAs of Land Plants." *Plant Cell* **19**(6): 1750-1769.
- Bang, S. W., D. K. Lee, H. Jung, P. J. Chung, Y. S. Kim, Y. D. Choi, J. W. Suh and J. K. Kim (2019). "Overexpression of OsTF1L, a rice HD-Zip transcription factor, promotes lignin biosynthesis and stomatal closure that improves drought tolerance." *Plant Biotechnol J* **17**(1): 118-131.
- Burke, M. B., D. B. Lobell and L. Guarino (2009). "Shifts in African crop climates by 2050, and the implications for crop improvement and genetic resources conservation." *Global Environmental Change* **19**(3): 317-325.
- Cao, J. F., B. Zhao, C. C. Huang, Z. W. Chen, T. Zhao, H. R. Liu, G. J. Hu, X. X. Shangguan, C. M. Shan, L. J. Wang, T. Z. Zhang, J. F. Wendel, X. Y. Guan and X. Y. Chen (2020). "The miR319-Targeted GhTCP4 Promotes the Transition from Cell Elongation to Wall Thickening in Cotton Fiber." *Mol Plant* **13**(7): 1063-1077.
- Chen and Xuemei (2009). "Small RNAs and Their Roles in Plant Development." *Annu Rev Cell Dev Biol* **2009**(1): 21-44.
- Clough, S. J. and A. F. Bent (1998). "Floral dip: a simplified method for Agrobacterium-mediated transformation of Arabidopsis thaliana." *Plant Journal* **16**(6): 735-743.
- Dong, J., N. Sun, J. Yang, Z. Deng, J. Lan, G. Qin, H. He, X. W. Deng, V. F. Irish, H. Chen and N. Wei (2019). "The Transcription Factors TCP4 and PIF3 Antagonistically Regulate Organ-Specific Light Induction of SAUR Genes to Modulate Cotyledon Opening during De-Etiolation in Arabidopsis." *The Plant cell* **31**(5): 1155-1170.
- Fan, D., L. Ran, J. Hu, X. Ye, D. Xu, J. Li, H. Su, X. Wang, S. Ren and K. Luo (2020). "miR319a/TCP module and DELLA protein regulate trichome initiation synergistically and improve insect defenses in Populus tomentosa." *New Phytol* **227**(3): 867-883.
- Fan, W., M. Zhang, H. Zhang and P. Zhang (2012). "Improved tolerance to various abiotic stresses in transgenic sweet potato (Ipomoea batatas) expressing spinach betaine aldehyde dehydrogenase." *PLoS One* **7**(5): e37344.
- Franco-Zorrilla, J. M., A. Valli, M. Todesco, I. Mateos, M. I. Puga, I. Rubio-Somoza, A. Leyva, D. Weigel, J. A. Garcia and J. Paz-Ares (2007). "Target mimicry provides a new mechanism for regulation of microRNA activity." *Nat Genet* **39**(8): 1033-1037.
- Hatfield, R. D., H. Jung, J. Ralph, D. R. Buxton and P. J. Weimer (1994). "A comparison of the insoluble residues produced by the Klason lignin and acid detergent lignin procedures." *Journal of the Science of Food and Agriculture* **65**(1): 51-58.
- He, Z., X. Zhao, F. Kong, Z. Zuo and X. Liu (2016). "TCP2 positively regulates HY5/HYH and photomorphogenesis in Arabidopsis." *J Exp Bot* **67**(3): 775-785.
- He, Z., X. Zhou, J. Chen, L. Yin, Z. Zeng, J. Xiang and S. Liu (2021). "Identification of a consensus DNA-binding site for the TCP domain transcription factor TCP2 and its important roles in the growth and development of Arabidopsis." *Mol Biol Rep* **48**(3): 2223-2233.
- Hirakawa, H., Y. Okada, H. Tabuchi, K. Shirasawa, A. Watanabe, H. Tsuruoka, C. Minami, S. Nakayama, S. Sasamoto, M. Kohara, Y. Kishida, T. Fujishiro, M. Kato, K. Nanri, A. Komaki, M. Yoshinaga, Y. Takahata, M. Tanaka, S. Tabata and S. N. Isobe (2015). "Survey of genome sequences in a wild sweet potato, Ipomoea trifida (H. B. K.) G. Don." *DNA Res* **22**(2): 171-179.
- Hu, H. and L. Xiong (2014). "Genetic engineering and breeding of drought-resistant crops." *Annu Rev Plant Biol* **65**: 715-741.
- Jin, R., B. H. Kim, C. Y. Ji, H. S. Kim, D. F. Ma and S.-S. Kwak (2017). "Overexpressing IbCBF3 increases low temperature and drought stress tolerance in transgenic sweetpotato." *Plant Physiology and Biochemistry* **118**: 45-54.
- Jones-Rhoades, M. W., D. P. Bartel and B. Bartel (2006). "MicroRNAs AND THEIR REGULATORY ROLES IN PLANTS." *Annual Review of Plant Biology* **57**(1): 19-53.
- Kang, C., S. He, H. Zhai, R. Li, N. Zhao and Q. Liu (2018). "A Sweetpotato Auxin Response Factor Gene (IbARF5) Is Involved in Carotenoid Biosynthesis and Salt and Drought Tolerance in Transgenic Arabidopsis." *Frontiers in Plant Science* **9**.
- Kang, C., H. Zhai, S. He, N. Zhao and Q. Liu (2019). "A novel sweetpotato bZIP transcription factor gene, IbbZIP1, is involved in salt and drought tolerance in transgenic Arabidopsis." *Plant Cell Reports* **38**(11): 1373-1382.
- Kuo, Y.-W., J.-S. Lin, Y.-C. Li, M.-Y. Jhu, Y.-C. King and S.-T. Jeng (2019). "MicroR408 regulates defense response upon wounding in sweet potato." *Journal of Experimental Botany* **70**(2): 469-483.
- Lee, Y. K., G. T. Kim, I. J. Kim, J. Park, S. S. Kwak, G. Choi and W. I. Chung (2006). "LONGIFOLIA1 and LONGIFOLIA2, two homologous genes, regulate longitudinal cell elongation in Arabidopsis." *Development* **133**(21): 4305-4314.
- Lee, Y. K. and I. J. Kim (2018). "Functional conservation of Arabidopsis LNG1 in tobacco relating to leaf shape change by increasing longitudinal cell elongation by overexpression." *Genes Genomics* **40**(10): 1053-1062.
- Lin, J.-S., C.-C. Lin, H.-H. Lin, Y.-C. Chen and S.-T. Jeng (2012). "MicroR828 regulates lignin and H2O2 accumulation in sweet potato on wounding." *New Phytologist* **196**(2): 427-440.
- Lin, K. H., C. M. Chiang, Y. C. Lai, S. H. You and H. F. Lo (2011). "Identification of Chilling-inducible Genes in Sweet potato by Suppression Subtractive Hybridization." *Research Journal of Biotechnology* **6**(2): 37-43.

26. Liu, Q., J. Liu, P. Zhang and S. He (2014). "Root and Tuber Crops - ScienceDirect." *Encyclopedia of Agriculture and Food Systems*: 46-61.
27. Liu, S., X. Mi, R. Zhang, Y. An, Q. Zhou, T. Yang, X. Xia, R. Guo, X. Wang and C. Wei (2019). "Integrated analysis of miRNAs and their targets reveals that miR319c/TCP2 regulates apical bud burst in tea plant (*Camellia sinensis*)." *Planta* **250**(4): 1111-1129.
28. Liu, W., Y. Jiang, C. Wang, L. Zhao, Y. Jin, Q. Xing, M. Li, T. Lv and H. Qi (2020). "Lignin synthesized by CmCAD2 and CmCAD3 in oriental melon (*Cucumis melo* L.) seedlings contributes to drought tolerance." *Plant Mol Biol* **103**(6): 689-704.
29. Liu, Y., D. Li, J. Yan, K. Wang, H. Luo and W. Zhang (2019). "MiR319-mediated ethylene biosynthesis, signalling and salt stress response in switchgrass." *Plant Biotechnology Journal* **17**(12): 2370-2383.
30. Livak, K. J. and T. D. Schmittgen (2001). "Analysis of relative gene expression data using real-time quantitative PCR and the 2(-Delta Delta C(T)) Method." *Methods* **25**(4): 402-408.
31. Long, Ruan, Lijuan, Chen, Yihong, Chen, Jinling, He, Wei and Zhang (2011). "Expression of Arabidopsis HOMEODOMAIN GLABROUS 11 Enhances Tolerance to Drought Stress in Transgenic Sweet Potato Plants." *Journal of Plant Biology* **55**(2): 151-158.
32. Matsuda, S., S. Takano, M. Sato, K. Furukawa, H. Nagasawa, S. Yoshikawa, J. Kasuga, Y. Tokuji, K. Yazaki, M. Nakazono, I. Takamure and K. Kato (2016). "Rice Stomatal Closure Requires Guard Cell Plasma Membrane ATP-Binding Cassette Transporter RCN1/OsABCG5." *Molecular Plant* **9**(3): 417-427.
33. Mbinda, W., C. Dixelius and R. Oduor (2019). "Induced Expression of Xerophyta viscosa XvSap1 Gene Enhances Drought Tolerance in Transgenic Sweet Potato." *Front Plant Sci* **10**: 1119.
34. Mbinda, W., O. Ombori, C. Dixelius and R. Oduor (2018). "Xerophyta viscosa Aldose Reductase, XvAld1, Enhances Drought Tolerance in Transgenic Sweetpotato." *Mol Biotechnol* **60**(3): 203-214.
35. Meng, X., G. Li, J. Yu, J. Cai, T. Dong, J. Sun, T. Xu, Z. Li, S. Pan, D. Ma and M. Zhu (2018). "Isolation, Expression Analysis, and Function Evaluation of 12 Novel Stress-Responsive Genes of NAC Transcription Factors in Sweetpotato." *Crop Science* **58**(3): 1328-1341.
36. Motsa, N. M., A. T. Modi and T. Mabhaudhi (2015). "Sweet potato (*Ipomoea batatas* L.) as a drought tolerant and food security crop." *South African Journal of ence* **111**(Number 11/12).
37. Moura, J., C. A. V. Bonine, J. D. F. Viana, M. C. Dornelas and P. Mazzafera (2010). "Abiotic and Biotic Stresses and Changes in the Lignin Content and Composition in Plants." *Journal of Integrative Plant Biology* **52**(4): 360-376.
38. Palatnik, J. F., E. Allen, X. Wu, C. Schommer, R. Schwab, J. C. Carrington and D. Weigel (2003). "Control of leaf morphogenesis by microRNAs." *Nature* **425**(6955): 257.
39. Pearce and RS (2001). "Plant freezing and damage." *ANN BOT* **2001,87**(4)(-): 417-424.
40. Pereira, Domingues, AP, Jansen, Choat and Mazzafera (2018). "Is embolism resistance in plant xylem associated with quantity and characteristics of lignin?" *TREES-STRUCT FUNCT* **2018,32**(2)(-): 349-358.
41. Ren, L., H. Wu, T. Zhang, X. Ge, T. Wang, W. Zhou, L. Zhang, D. Ma and A. Wang (2021). "Genome-Wide Identification of TCP Transcription Factors Family in Sweet Potato Reveals Significant Roles of miR319-Targeted TCPs in Leaf Anatomical Morphology." *Frontiers in Plant Science* **12**(1431).
42. Sato, Y., T. Murakami, H. Funatsuki, S. Matsuba, H. Saruyama and M. Tanida (2001). "Heat shock-mediated APX gene expression and protection against chilling injury in rice seedlings." *JOURNAL OF EXPERIMENTAL BOTANY*.
43. Schommer, C., J. M. Debernardi, E. G. Bresso, R. E. Rodriguez and J. F. Palatnik (2014). "Repression of Cell Proliferation by miR319-Regulated TCP4." *Molecular Plant* **7**(10): 1533-1544.
44. Schommer, C., J. F. Palatnik, P. Aggarwal, A. Chetelat, P. Cubas, E. E. Farmer, U. Nath and D. Weigel (2008). "Control of jasmonate biosynthesis and senescence by miR319 targets." *Plos Biology* **6**(9): 1991-2001.
45. Shi, X., F. Jiang, J. Wen and Z. Wu (2019). "Overexpression of Solanum habrochaites microRNA319d (sha-miR319d) confers chilling and heat stress tolerance in tomato (*S. lycopersicum*)." *BMC Plant Biol* **19**(1): 214.
46. Stortenbeker, N. and M. Bemer (2019). "The SAUR gene family: the plant's toolbox for adaptation of growth and development." *J Exp Bot* **70**(1): 17-27.
47. Sun-ting, W., S. Xiao-li, H. Yoichiro, Y. Yang, J. Bei, S. Zhong-wen, S. Ming-zhe, D. Xiang-bo, Z. Yan-ming and U. Turgay (2014). "MicroRNA319 Positively Regulates Cold Tolerance by Targeting OsPCF6 and OsTCP21 in Rice (*Oryza sativa* L.)." *Plos One* **9**(3): e91357.
48. Sun, S. C., X. P. Xiong, X. L. Zhang, H. J. Feng, Q. H. Zhu, J. Sun and Y. J. Li (2020). "Characterization of the Gh4CL gene family reveals a role of Gh4CL7 in drought tolerance." *BMC Plant Biol* **20**(1): 125.
49. Sun, X., C. Wang, N. Xiang, X. Li, S. Yang, J. Du, Y. Yang and Y. Yang (2017). "Activation of secondary cell wall biosynthesis by miR319-targeted TCP4 transcription factor." *Plant Biotechnol J* **15**(10): 1284-1294.
50. Sunkar and R. (2004). "Novel and Stress-Regulated MicroRNAs and Other Small RNAs from Arabidopsis." *Plant Cell* **16**(8): 2001-2019.
51. Taylor, R. S., J. E. Tarver, S. J. Hiscock and P. C. J. Donoghue (2014). "Evolutionary history of plant microRNAs." *Trends in Plant Science* **19**(3): 175-182.

52. Tsukaya, H. (2005). "Leaf shape: genetic controls and environmental factors." *Int J Dev Biol* **49**(5-6): 547-555.
53. Vadde, B. V. L., K. R. Challa, P. Sunkara, A. S. Hegde and U. Nath (2019). "The TCP4 Transcription Factor Directly Activates TRICHOMELESS1 and 2 and Suppresses Trichome Initiation." *Plant Physiology* **181**(4): 1587-1599.
54. Wang, A. M., M. K. Zhu, Y. H. Luo, Y. J. Liu, R. S. Li, M. Kou, X. Wang, Y. G. Zhang, X. Q. Meng, Y. L. Zheng and D. F. Ma (2017). "A sweet potato cinnamate 4-hydroxylase gene, IbC4H, increases phenolics content and enhances drought tolerance in tobacco." *Acta Physiologiae Plantarum* **39**(12).
55. Wang, B., H. Zhai, S. Z. He, H. Zhang, Z. T. Ren, D. D. Zhang and Q. C. Liu (2016). "A vacuolar Na⁺/H⁺ antiporter gene, IbNHX2, enhances salt and drought tolerance in transgenic sweetpotato." *Scientia Horticulturae* **201**: 153-166.
56. Wang, F., Z. Tao, G. Wu, C. Lang, Z. Hu, J. Shi, J. Wei, J. Chen and R. Liu (2015). "Overexpression of miR319a Affects the Balance Between Mitosis and Endoreduplication in Arabidopsis Leaves." *Plant Molecular Biology Reporter* **33**(6): 1-8.
57. Wang, J., N. Sun, F. Zhang, R. Yu, H. Chen, X. W. Deng and N. Wei (2020). "SAUR17 and SAUR50 Differentially Regulate PP2C-D1 during Apical Hook Development and Cotyledon Opening in Arabidopsis." *Plant Cell* **32**(12): 3792-3811.
58. Wang, W., X. Qiu, Y. Yang, H. S. Kim, X. Jia, H. Yu and S. S. Kwak (2019). "Sweetpotato bZIP Transcription Factor IbABF4 Confers Tolerance to Multiple Abiotic Stresses." *Front Plant Sci* **10**: 630.
59. Weng, S.-T., Y.-W. Kuo, Y.-C. King, H.-H. Lin, P.-Y. Tu, K.-S. Tung and S.-T. Jeng (2020). "Regulation of microRNA2111 and its target IbFBK in sweet potato on wounding." *Plant Science* **292**.
60. Xie, Q., X. Liu, Y. Zhang, J. Tang, D. Yin, B. Fan, L. Zhu, L. Han, G. Song and D. Li (2017). "Identification and Characterization of microRNA319a and Its Putative Target Gene, PvPCF5, in the Bioenergy Grass Switchgrass (*Panicum virgatum*)." *Front Plant Sci* **8**: 396.
61. Xie, Z., A. Wang, H. Li, J. Yu, J. Jiang, Z. Tang, D. Ma, B. Zhang, Y. Han and Z. Li (2017). "High throughput deep sequencing reveals the important roles of microRNAs during sweetpotato storage at chilling temperature." *Scientific Reports* **7**(1): 16578.
62. Xu, W., W. Tang, C. Wang, L. Ge, J. Sun, X. Qi, Z. He, Y. Zhou, J. Chen, Z. Xu, Y. Z. Ma and M. Chen (2020). "SiMYB56 Confers Drought Stress Tolerance in Transgenic Rice by Regulating Lignin Biosynthesis and ABA Signaling Pathway." *Front Plant Sci* **11**: 785.
63. Yang, L. Dayong, M. Donghai, L. Xue, J. Chengjun, L. Xiaobing, Z. Xianfeng, C. Zhukuan, C. Caiyan and Z. Lihuang (2013). "Overexpression of microRNA319 impacts leaf morphogenesis and leads to enhanced cold tolerance in rice (*Oryza sativa* L.)." *Plant Cell & Environment* **36**(12): 2207-2218.
64. Yang, C., D. Li, D. Mao, X. Liu, C. Ji, X. Li, X. Zhao, Z. Cheng, C. Chen and L. Zhu (2013). "Overexpression of microRNA319 impacts leaf morphogenesis and leads to enhanced cold tolerance in rice (*Oryza sativa* L.)." *Plant Cell Environ* **36**(12): 2207-2218.
65. Yang, J., H.-P. Bi, W.-J. Fan, M. Zhang, H.-X. Wang and P. Zhang (2011). "Efficient embryogenic suspension culturing and rapid transformation of a range of elite genotypes of sweet potato (*Ipomoea batatas* [L.] Lam.)." *Plant Science* **181**(6): 701-711.
66. Zhai, H., F. Wang, Z. Si, J. Huo, L. Xing, Y. An, S. He and Q. Liu (2016). "A myo-inositol-1-phosphate synthase gene, IbMIPS1, enhances salt and drought tolerance and stem nematode resistance in transgenic sweet potato." *Plant Biotechnol J* **14**(2): 592-602.
67. Zhao, D., Y. Luan, W. Shi, X. Zhang, J. Meng and J. Tao (2021). "A *Paeonia ostii* caffeoyl-CoA O-methyltransferase confers drought stress tolerance by promoting lignin synthesis and ROS scavenging." *Plant Sci* **303**: 110765.
68. Zhou, M., D. Li, Z. Li, Q. Hu, C. Yang, L. Zhu and H. Luo (2014). "Constitutive expression of a miR319 gene alters plant development and enhances salt and drought tolerance in transgenic creeping bentgrass." *Plant Physiology* **161**(4): 1375-1391.
69. Zhou, Y., H. Zhai, S. He, H. Zhu, S. Gao, S. Xing, Z. Wei, N. Zhao and Q. Liu (2020). "The Sweetpotato BTB-TAZ Protein Gene, IbBT4, Enhances Drought Tolerance in Transgenic Arabidopsis." *Frontiers in Plant Science* **11**.
70. Zhou, Y. Y., H. Zhu, S. Z. He, H. Zhai, N. Zhao, S. H. Xing, Z. H. Wei and Q. C. Liu (2019). "A Novel Sweetpotato Transcription Factor Gene IbMYB116 Enhances Drought Tolerance in Transgenic Arabidopsis." *Frontiers in Plant Science* **10**.
71. Zou, J. J., Z. Y. Zheng, S. Xue, H. H. Li, Y. R. Wang and J. Le (2016). "The role of Arabidopsis Actin-Related Protein 3 in amyloplast sedimentation and polar auxin transport in root gravitropism." *J Exp Bot* **67**(18): 5325-5337